



Progression of Capillary Hypoperfusion in Advanced Stages of Nonproliferative Diabetic Retinopathy: 6-month Analysis of RICHARD Study

Inês Pereira Marques, MD, PhD,^{1,2,3} Débora Reste-Ferreira, MSc,¹ Torcato Santos,¹ Luís Mendes, PhD,¹ António Cunha-Vaz Martinho, MD,^{1,4} Taffeta Ching Ning Yamaguchi, PhD,⁵ Ana Rita Santos, PhD,^{1,2,6} Elizabeth Pearce, PhD,⁷ José Cunha-Vaz, MD, PhD^{1,8}

Purpose: To evaluate the 6-month progression of retinal capillary perfusion in eyes with advanced stages of nonproliferative diabetic retinopathy (NPDR).

Design: RICHARD (NCT05112445), 2-year prospective longitudinal study.

Participants: Sixty eyes with Diabetic Retinopathy Severity Scale (DRSS) levels 43, 47, and 53 from 60 patients with type 2 diabetes. Fifty-one patients completed the 6-month evaluation.

Methods: Eyes were evaluated on Optos California (Optos plc) ultrawidefield fundus fluorescein angiography (UWF-FFA), swept-source OCT angiography (SS-OCTA) (PLEX Elite 9000, ZEISS) and spectral-domain OCTA (SD-OCTA) (CIRRUS HD-OCT 5000 Angioplex, ZEISS). DRSS classification was performed based on 7-field color fundus photographs (CFPs) complemented with Optos California UWF-fundus imaging.

Main Outcome Measures: Ischemic index was obtained from Optos. Vascular quantification metrics, namely foveal avascular zone, skeletonized vessel density (SVD), and perfusion density (PD) metrics, were acquired on OCTA in the superficial and deep capillary plexuses (SCP and DCP). Microaneurysm assessment was automatically performed based on CFP images using the RetmarkerDR (Retmarker SA, Meteda Group).

Results: Swept-source-OCTA metrics showed statistically significant differences between the advanced stages of NPDR. Differences between DRSS levels 47 and 53 were found at baseline in the inner ring (SVD, SCP: $P = 0.005$ and DCP: $P = 0.042$ and PD, SCP: $P = 0.003$) and outer ring (SVD, SCP: $P = 0.007$ and DCP: $P = 0.030$ and PD, SCP: $P = 0.020$ and DCP: $P = 0.025$). No significant differences were observed at baseline between DRSS levels 43 and 47. In SD-OCTA, the differences were similar but did not reach statistical significance. The total ischemic index showed an increase in association with diabetic retinopathy (DR) severity, but the differences between DRSS levels did not reach statistical significance. The number of microaneurysms also increased significantly with DR severity ($P = 0.033$). Statistically significant 6-month progression was detected with SS-OCTA in eyes with DRSS levels 47 and 53 but not in DRSS level 43. In eyes with DRSS level 53, 6-month progression was identified using a combination of metrics of capillary nonperfusion and microaneurysm counts.

Conclusions: In a 6-month period, significant microvascular disease progression can be identified in eyes with DRSS levels 47 and 53 by performing OCTA examinations and microaneurysm counting using CFP.

Financial Disclosure(s): Proprietary or commercial disclosure may be found in the Footnotes and Disclosures at the end of this article. *Ophthalmology Science* 2025;5:100632 © 2024 by the American Academy of Ophthalmology. This is an open access article under the CC BY-NC-ND license (<http://creativecommons.org/licenses/by-nc-nd/4.0/>).

Diabetic retinopathy (DR), the most common microvascular complication of diabetes, is the leading cause of vision loss in adults.^{1,2} The International Diabetes Federation estimated that by 2045 there will be 783 million people worldwide with diabetes.³ Approximately one third of people with diabetes develop signs of DR, with 10% developing vision-threatening complications.^{2,4,5} It is, therefore, crucial to identify the eyes of people with diabetes that are at high risk of vision loss.

Retinal capillary hypoperfusion in the central retina is a key hallmark of rapid progression of nonproliferative DR (NPDR) to sight-threatening complications, clinically

significant macular edema (CSME) and proliferative DR (PDR).^{6–9} However, peripheral changes need to be considered and may be predominant in some eyes.^{10,11} It is particularly important to identify eyes with increased levels of hypoperfusion, corresponding to the ischemia phenotype characterized by decrease of skeletonized vessel density (SVD) in the retinal superficial capillary plexus (SCP), that is, decreased values of SVD in SCP ≥ 2 SD of healthy controls values. Our group has previously proposed the ischemic phenotype associated with risk for severity progression.^{8,12,13}

Multiple imaging modalities such as dilated fundus examination, color fundus photography (CFP), ultrawidefield color fundus photography (UWF-FP), fundus fluorescein angiography (FFA), OCT, and OCT angiography (OCTA) are currently used for diagnosing and staging DR. The most informative and gold standard method for diagnosing DR over the years was FFA, offering detailed information about retinal vascular integrity.¹⁴ However, this imaging procedure requires the administration of fluorescent dye-based invasive test presenting several risks and contraindications and does not allow visualization of the deep capillary plexus (DCP).¹⁵

Examination techniques without the use of injectable dyes are becoming more widely available. In recent years, noninvasive imaging modalities have been introduced into the clinical practice, allowing improved visibility of the retinal vascular structures.¹⁶ Swept-source OCT angiography (SS-OCTA) provide noninvasive 3-dimensional mapping of the retinal microvasculature allowing the quantification of retinal capillary hypoperfusion over larger field of view with deeper light penetration,¹⁷ thus offering additional information to spectral-domain OCTA. In fact, although OCTA devices rely on the common principle that erythrocytes could be used as a motion contrast to differentiate vessels from static tissues, they use different algorithms for image acquisition and processing and different methods for layer segmentation. Furthermore, OCTA images provide for the first-time identification of the deep retinal capillaries, allowing a better understanding of the pathophysiological changes in DR. A multimodal imaging approach allows examination of the prevalence of different disease pathways in the initial stages of the disease and can potentially clarify the risk of progression in different patients.¹²

Associated with disease progression and ischemia, other lesions such as microaneurysms (MAs) and intraretinal microvascular abnormalities (IRMAs) are considered to play an important role and need to be further evaluated in association with ischemic changes. Automated image analysis of MA turnover, performed on CFP images with RetmarkerDR software, is a noninvasive technique with proven ability to identify eyes that are at risk of DR progression.^{18,19} To address these changes with potential effective therapies, it is crucial to understand disease progression and identify the metrics that can be used to plan the necessary clinical trials.

The aim of this study is to evaluate the initial 6-month progression of retinal capillary perfusion in eyes with advanced stages of NPDR focusing on Diabetic Retinopathy Severity Scale (DRSS) levels 43, 47, and 53 using a multimodal approach by combining different examination procedures.

Methods

The RICHARD study (NCT05112445, clinicaltrials.gov identifier) is a noninterventive prospective cohort study with 2 years of follow-up period and adheres to the tenets of the Declaration of Helsinki. This study was reviewed and approved by the Association for Innovation and Biomedical Research on Light and Image

Ethics Committee and was conducted in accordance with the legislation and institutional requirements. The participants provided their written informed consent to participate in this study.

Inclusion and Exclusion Criteria

Eligible patients met the following inclusion criteria: (1) type 2 diabetes according to World Health Organization; (2) patients over 18 years of age; (3) DRSS levels between 43 and 53 based on the ETDRS criteria complemented with UWF-FP imaging; (4) refraction with a spherical equivalent <5 diopters; and (5) able to provide informed consent. Exclusion criteria were as follows: any retinal vascular disease that may interfere with study results (including CSME), glaucoma, age-related macular degeneration, vitreomacular disease, any eye surgery within a period of 6 months before the baseline visit, previous laser treatment or intravitreal injections, dilation of pupil <5 mm and uncontrolled glycated hemoglobin A1C level $>12\%$ (107.66 mmol/mol). Only 1 eye per patient was included. The eye with more severe DRSS grading was chosen. However, when both eyes had the same DRSS level, the eye with the higher ischemic index on UWF-FFA was chosen.

Subjects

Sixty eyes with advanced stages of NPDR (DRSS levels 43, 47, and 53) from 60 patients with type 2 diabetes were considered eligible for baseline analysis. However, only 51 patients/eyes completed the 2 examinations with an interval of 6 months (6-month), because 1 developed PDR, 1 developed CSME, 5 missed the second visit, and 2 withdrew consent.

Clinical and Ophthalmological Examinations

Demographic and clinical information for all participants including age, sex, diabetes duration, vital signs (height, weight, body mass index, systolic and diastolic blood pressure, and heart rate) and laboratory characteristics (glycated hemoglobin, cholesterol, and triglycerides) were recorded at baseline. All participants underwent comprehensive ophthalmological examination, including best-corrected visual acuity (BCVA) evaluation, slit-lamp bio-microscopy, indirect ophthalmoscopy, intraocular pressure measurement and fundus imaging. OCT angiography images were acquired with 2 different devices (swept-source OCTA [SS-OCTA] and spectral-domain OCTA [SD-OCTA]).

BCVA Evaluation

Best-corrected visual acuity was evaluated at 4 meters distance using the ETDRS chart.²⁰ Best-corrected visual acuity letters score was calculated by adding the number of letters read at 4 meters plus the 30 letters read at 1 meter. Best-corrected visual acuity was evaluated both at baseline and at 6 months.

DRSS

Diabetic Retinopathy Severity Scale grading was performed at baseline based on the grading of standard 7-field CFP images obtained with 35° field of view using the Topcon TRC 50DX mydriatic retinal camera (Topcon Medical Systems), with a resolution of 3596 × 2448 pixels. Adequate dilation of the pupil of at least 6 mm was ensured using mydriasis (0.5 % tropicamide and 0.5% phenylephrine hydrochloride topical drops) to obtain good quality images.²¹ In addition, we complemented the classification with the UWF-FP images captured using the UWF Optos California (Optos plc). This device's software automatically places a grid to outline the 7 ETDRS fields.^{22,23} Retinal photographs were evaluated by 2 certified graders at the Coimbra Ophthalmology

Reading Centre and were classified according to DRSS. In the case of a discrepancy between the 2 retinal specialists, a senior grader provided adjudication. The DRSS was classified as moderate NPDR DRSS level 43, moderately severe NPDR DRSS level 47, and severe NPDR DRSS level 53.

UWF-FFA

Ultrawidefield FFA images were captured using the Optos California device (Optos plc). This system is a confocal scanning laser ophthalmoscope with an ellipsoidal mirror able to capture 130° of the retinal fundus in a single image without requiring bright illumination lighting or a contact lens and, in some patients, pupillary dilation. This device uses a blue argon laser at 488 nm to excite sodium fluorescein and captures a 4000 × 4000-pixel image through a 500-nm barrier filter. This single scan takes 0.25 seconds to provide approximately 20-pixel resolution per degree.^{24,25} Fundus fluorescein angiography requires the intravenous injection of the fluorescein dye. Patients were injected with 1.5 ml of 100 mg/ml (20%) sodium fluorescein and early phase images were analyzed to calculate the percentage of total ischemic index and leakage index and also to identify IRMA. Ischemic index percentage is obtained by the total area of retinal ischemia divided by total area of visible retina.²⁶ Fundus fluorescein angiography was performed only at baseline visit.

OCT

Structural metrics such as central retinal thickness and ganglion cell layer plus inner plexiform layers (GCL + IPL) thickness were measured on each participant at each visit (baseline and 6-month visit) using OCT acquisition protocol Macular Cube 512 × 128. This acquisition protocol, available on the Cirrus HD-OCT 5000 Angioplex (ZEISS), consists of 128 B-scans with 512 A-scans each. Central retinal thickness, defined as the average of retinal thickness in the central subfield, is an objective quantification of edema. The GCL + IPL thickness, defined as the average layer thickness in the 0.5-mm to 2-mm annulus centered on fovea, is an objective quantification of neurodegenerative changes.

SD-OCTA

All participants were imaged with Cirrus Zeiss 5000 Angioplex (ZEISS) SD-OCTA device using the Angiography 3 × 3 mm and Angiography 6 × 6-mm acquisition protocols at each visit (baseline and 6 month visit). The Angiography 6 × 6 mm acquisition protocol, consisting of 350 clusters of 2 B-scans repetitions with 350 A-scans, provides wider field of view but lower digital sampling when comparing to the Angiography 3 × 3 mm acquisition protocols which consists of 245 clusters of 4 B-scans repetitions with 245 A-scans.

Acquisition data were exported from the ophthalmological device and processed through the Carl Zeiss Meditec Density Exerciser (version:10.0.12787; Carl Zeiss Meditec, Inc) to compute slab images and numerical data for the foveal avascular zone, the SVD and perfusion density (PD) metrics at the SCP and DCP. Perfusion density metrics and images are the result of the binarization of the en face angiography images and represent changes in vessel perfusion, namely, capillary vasodilation or vasoconstriction. A skeletonization of the binary images generates the SVD metrics and images to represent the number of individual

capillaries that are carrying red blood cells. Its decrease indicates capillary closure.^{27,28}

Skeletonized vessel density and PD were measured in the macular area (20° of the retina): central subfield (0–0.5-mm radius ring centered at the fovea), inner ring (0.5–1.5-mm radius ring centered at the fovea) and outer ring (1.5–3.0-mm radius ring centered at the fovea).

SS-OCTA

Images from patients were acquired using the Angio 6-mm × 6-mm acquisition protocol available in the PLEX Elite 9000 (ZEISS) at each visit (baseline and 6-month visit). This SS-OCTA operates a tunable 1060-nm laser to provide an axial resolution of 6.3 μm. Angio 6-mm × 6-mm acquisition protocol is able to scan 20° of the retina and provides angiography slabs images based on 2 repetitions of 500 B-scans with 500 A-scans with an acquisition rate of 100 000 A-scans/second. Although with a lower axial resolution than the SD-OCTA, this device provides increased definition of the DCP because of higher penetration of the laser source.^{29–31}

Acquired data from this device were then processed using the “Macular Density v0.7.3.3” analysis protocol available on the Advanced Retina Imaging Network Hub (<https://arinetworkhub.com>). This analysis algorithm provides slabs images for the SCP, DCP, and total retinal slabs, and SVD and PD numerical data similar to those reported for the SD-OCTA device.³² Skeletonized vessel density and PD were also measured in the inner and outer rings of the retina.

OCTA Quality Images

All OCT and OCTA examinations were reviewed for quality assessment. Foveal avascular zone measurements with poor delimitation were discarded from the analysis. In addition, the grader reviewed each inner/outer ring quadrants for the SCP and DCP to ensure reliable metrics. Criteria for measurement reliability for SD-OCTA were well-focused capillary networks and absence of cropped scans, vessel duplication, and opaque artifacts. Single low-quality inner/outer ring quadrants were not considered in the analysis. If >1 inner ring quadrant was classified as low-quality, then corresponding ring measurements for that slab were discarded. For SS-OCTA, the vascular metrics were considered if no defocus or other artifacts were absent in >80% of the image.

Microaneurysm Detection

Microaneurysm identification was automatically performed on CFP images (50° of the retina - field F2) using the RetmarkerDR software (Retmarker SA, Meteda Group), a computer-aided diagnostic software that performs MA earmarking and identification of macular red dot-like vascular lesions.^{33,34} It allows the comparison of lesions within the same retinal location between different visits. Likewise, this algorithm computes the number and localization of MA in each visit (baseline and 6-month visit) and the number of MA that appear and disappear from one visit to the other, allowing the calculation of the MA disappearance and MA formation rates between visits. Microaneurysm turnover is computed as the sum of the MA formation rate

and MA disappearance rate. RetmarkerDR has been used since 2011, and RetmarkerDR Biomarker is currently certified as a class IIA medical device in Europe. RetmarkerDR software is highly conservative to reduce variability.

IRMA Identification

Intraretinal microvascular abnormalities were defined by ETDRS Research Group in 1991 as tortuous intraretinal vascular segments, varying in caliber from barely visible to 31 μm per the ETDRS.²¹ In this analysis, IRMAs were identified as capillary tortuosities covering a minimum equivalent circular area of 300 μm calculated to correspond to ETDRS standard photo 8A. Multimodal imaging was performed at baseline to identify IRMA, including CFP (up to 50° of the retina), UWF-FFA (up to 130° of the retina), and SS-OCTA devices (up to 50° of the retina). In addition, we compare the presence of IRMAs in the 6-month interval identified only by SS-OCTA. Three different zones of the retina were examined: central macula (up to 20° of the retina), posterior pole (up to 50° of the retina), and mid- and far-periphery (up to 130° of the retina).

Statistical Analysis

Statistical analyses of the data were performed using STATA software, version 16.1 (StataCorp LLC). *P* values <0.05 were considered statistically significant different.

Distribution of data normality was assessed using the Kolmogorov–Smirnov test. Numerical variables were expressed as the average and standard deviation. Percentages were reported for categorical variables, and the chi-square test were used to compare differences between the DRSS groups.

The Mann-Whitney *U* test, a nonparametric statistical test, was performed to compare the differences between DRSS groups for clinical and ophthalmological characteristics (DRSS level 43 vs. DRSS level 47 vs. DRSS level 53). The Wilcoxon signed rank test, a nonparametric paired test, was used to evaluate the progression of microvascular metrics between an interval of 6-month (baseline vs. 6-month).

Linear mixed models were applied to evaluate the correlation between microaneurysm turnover and microvascular related variables. Visit, DRSS levels, and microvascular related variables were used as continuous fixed variables. The estimated effects of the predicting variables were described by beta coefficients with 95% confidence intervals. The patients were used as a random effect (intercept only).

Results

Sixty eyes with moderate to severe NPDR (DRSS levels 43, 47, and 53) from 60 patients with type 2 diabetes were included in the RICHARD study. The mean age of all patients was 67.78 ± 8.64 years, with 78% being male. At the baseline visit, there were 12 eyes (20%) classified as DRSS level 43 (moderate NPDR), 36 eyes (60%) classified as DRSS level 47 (moderately severe NPDR), and 12 eyes (20%) classified as DRSS level 53 (severe NPDR).

Of the 60 eyes included at baseline, all eyes classified as DRSS level 43 at baseline completed the 6-month evaluation. Six eyes classified at baseline as DRSS level 47 (6 out of 36 eyes) were not available for the 6-month visit due to development of PDR (1), 4 missed the second visit and 1 withdrew consent. Three eyes classified at baseline as DRSS level 53 (3 out of 12 eyes) were not available for the second visit because 1 developed CSME, 1 missed the second visit, and 1 withdrew consent.

Baseline Analysis

Demographic characteristics, vital signs, and laboratory characteristics of the 60 patients at baseline according to DR severity levels are described in Table 1. No statistically significant differences were found between DRSS levels, except for the diastolic blood pressure (43 vs. 53: *P* = 0.044 and 47 vs. 53: *P* = 0.011).

Ophthalmological examinations at baseline according to DRSS levels are also reported in Table 1. No statistically significant differences for BCVA and intraocular pressure were observed between the eyes with advanced stages of NPDR. However, the total ischemic index obtained from UWF-FFA showed an increase in association with DR severity although the differences between them did not reach statistical significance (DRSS level 43: 2.97 ± 2.61 ; DRSS level 47: 3.69 ± 4.86 ; DRSS level 53: 3.95 ± 2.80). In addition, the GCL + IPL thickness obtained from SD-OCT also showed a decrease in association with DR severity but did not reach statistical significance (DRSS level 43: 81.08 ± 10.16 ; DRSS level 47: 76.28 ± 11.11 ; DRSS level 53: 72.00 ± 15.33).

When evaluating the microvascular metrics using the SS-OCTA (6 × 6-mm acquisition protocol), differences between DRSS levels 47 and 53 were found in the inner ring (SVD, SCP: *P* = 0.005 and DCP: *P* = 0.042 and PD, SCP: *P* = 0.003) and in the outer ring (SVD, SCP: *P* = 0.007 and DCP: *P* = 0.030 and PD, SCP: *P* = 0.020 and DCP: *P* = 0.025). No statistically significant differences were observed in SS-OCTA metrics between DRSS levels 43 and 47. In the SD-OCTA, the microvascular changes between DR severity levels were similar but did not reach statistical significance, suggesting that SD-OCTA may have less discriminatory power between DRSS levels.

Our results also show that the number of MAs increased with increased DR severity (43 vs. 53: *P* = 0.002 and 47 and 53: *P* = 0.033, Table 1). Multimodal imaging was performed to identify IRMAs at baseline, including UWF-FFA (up to 130° area), CFP (up to 50° area), and 2 different OCTA devices (SS-OCTA: up to 50° area and SD-OCTA: up to 20° area). Intraretinal microvascular abnormalities were identified throughout the retina in DRSS levels 47 and 53, whereas in DRSS level 43 IRMAs were detected only in areas outside the central macula (FoV >20°). Furthermore, UWF-FFA was capable of detecting IRMAs in the mid- and far-periphery (FoV >50°). In addition, the number of IRMAs identified by different modalities are present in increased numbers with increased DR severity.

Table 1. Clinical and Ophthalmological Characteristics at Baseline According to DR Severity Levels

	DRSS Level 43	DRSS Level 47	DRSS Level 53	P Value		
	n = 12	n = 36	n = 12	43 vs. 47	43 vs. 53	47 vs. 53
Demographic characteristics						
Sex						
Male	11 (91.7%)	27 (75.0%)	9 (75.0%)	0.212	0.295	0.638
Female	1 (8.3%)	9 (25.0%)	3 (25.0%)			
Age (yrs), mean ± SD	66.33 ± 8.99	68.69 ± 7.88	66.50 ± 11.04	0.608	0.943	0.399
Diabetes duration (yrs), mean ± SD	21.67 ± 7.05	22.42 ± 9.27	20.67 ± 7.29	0.818	0.854	0.755
Vital signs, mean ± SD						
Height (cm)	164.42 ± 6.88	164.92 ± 9.13	162.17 ± 3.71	0.800	0.123	0.139
Weight (kg)	80.79 ± 11.16	80.15 ± 13.05	76.42 ± 13.27	0.694	0.310	0.313
Body mass index (kg/m ²)	30.07 ± 5.34	29.49 ± 4.26	29.03 ± 4.75	0.949	0.619	0.576
Systolic blood pressure (mmHg)	137.67 ± 12.17	138.78 ± 12.74	142.58 ± 7.57	0.600	0.353	0.600
Diastolic blood pressure (mmHg)	70.75 ± 8.96	72.94 ± 6.67	77.67 ± 4.10	0.668	0.044*	0.011*
Heart rate (bpm)	73.50 ± 11.09	70.92 ± 11.32	75.83 ± 8.73	0.576	0.504	0.160
Laboratory characteristics, mean ± SD						
HbA1c (%)	7.62 ± 1.01	7.59 ± 0.90	7.21 ± 1.47	0.828	0.417	0.130
Total cholesterol (mg/dL)	148.17 ± 41.13	167.58 ± 40.32	171.83 ± 71.06	0.113	0.478	0.902
LDL cholesterol (mg/dL)	77.58 ± 31.64	89.67 ± 33.70	92.75 ± 55.20	0.380	0.442	0.883
HDL cholesterol (mg/dL)	47.75 ± 12.49	48.83 ± 14.72	48.33 ± 14.08	0.874	0.599	0.948
Triglycerides (mg/dL)	117.00 ± 33.26	145.42 ± 67.58	154.83 ± 74.91	0.254	0.340	0.874
Ophthalmological examinations, mean ± SD						
Best-corrected visual acuity (letters)	84.92 ± 5.26	82.08 ± 5.07	84.58 ± 5.09	0.067	0.674	0.110
Intraocular pressure (mmHg)	17.00 ± 2.89	16.81 ± 3.28	17.08 ± 4.70	0.782	1.000	0.719
UWF-FFA						
Ischemic index, %	2.97 ± 2.61	3.69 ± 4.86	3.95 ± 2.80	0.799	0.449	0.319
Leakage index, %	1.70 ± 2.50	2.11 ± 4.61	2.36 ± 2.53	0.729	0.418	0.212
SD-OCT						
CRT – average CSF (μm)	275.00 ± 24.68	275.69 ± 28.68	275.92 ± 17.36	0.521	0.640	0.651
GCL + IPL thickness (μm)	81.08 ± 10.16	76.28 ± 11.11	72.00 ± 15.33	0.167	0.075	0.318
SS-OCTA (6 × 6 mm acquisition protocol)						
FAZ area (mm ²)	0.36 ± 0.25	0.29 ± 0.14	0.24 ± 0.11	0.681	0.347	0.233
FAZ length (mm)	2.63 ± 1.19	2.27 ± 0.67	2.10 ± 0.55	0.810	0.410	0.441
FAZ circularity (a.u.)	0.65 ± 0.14	0.69 ± 0.10	0.68 ± 0.11	0.364	0.977	0.716
Skeletonized vessel density – MAC – SCP (mm ⁻¹)	17.89 ± 2.46	17.68 ± 1.64	19.08 ± 1.10	0.283	0.079	0.007*
Skeletonized vessel density – MAC – DCP (mm ⁻¹)	10.41 ± 3.58	9.64 ± 3.28	12.13 ± 2.60	0.403	0.211	0.026*
Skeletonized vessel density – InR – SCP (mm ⁻¹)	17.57 ± 3.33	17.90 ± 1.80	19.46 ± 1.14	0.597	0.079	0.005*
Skeletonized vessel density – InR – DCP (mm ⁻¹)	10.21 ± 4.11	10.44 ± 3.54	12.73 ± 2.03	0.860	0.134	0.042*
Skeletonized vessel density – OutR – SCP (mm ⁻¹)	18.33 ± 2.21	17.92 ± 1.68	19.28 ± 1.17	0.252	0.169	0.007*
Skeletonized vessel density – OutR – DCP (mm ⁻¹)	10.85 ± 3.66	9.75 ± 3.42	12.37 ± 2.90	0.242	0.347	0.030*
Perfusion density – MAC – SCP (a.u.)	0.40 ± 0.06	0.39 ± 0.04	0.42 ± 0.02	0.305	0.151	0.007*
Perfusion density – MAC – DCP (a.u.)	0.21 ± 0.07	0.20 ± 0.07	0.25 ± 0.06	0.488	0.211	0.026*
Perfusion density – InR – SCP (a.u.)	0.38 ± 0.07	0.39 ± 0.04	0.42 ± 0.02	0.630	0.044*	0.003*
Perfusion density – InR – DCP (a.u.)	0.20 ± 0.08	0.21 ± 0.07	0.26 ± 0.04	0.769	0.079	0.051
Perfusion density – OutR – SCP (a.u.)	0.41 ± 0.05	0.40 ± 0.04	0.43 ± 0.02	0.262	0.316	0.020*
Perfusion density – OutR – DCP (a.u.)	0.22 ± 0.08	0.20 ± 0.07	0.25 ± 0.06	0.214	0.379	0.025*
RetmarkerDR from CFP images (Field 2)						
Number of microaneurysms	2.92±2.54	6.61±6.54	13.25±11.77	0.053	0.002*	0.033*

a.u. = arbitrary units; CFP = color fundus photography; CRT = central retinal thickness; CSF = central subfield; DCP = deep capillary plexus; DRSS = Diabetic Retinopathy Severity Scale; FAZ = foveal avascular zone; GCL + IPL = ganglion cell layer + inner plexiform layer; HbA1c = glycated hemoglobin; HDL = high-density lipoprotein; InR = inner ring; SD = standard deviation; LDL = low-density lipoprotein; MAC = macular area (20°); OutR = outer ring; SCP = superficial capillary plexus; SD = standard deviation; SD-OCT = spectral-domain OCT; SS-OCTA = swept-source OCT angiography; UWF-FFA = ultrawide field fundus fluorescein angiography.

*Values represent statistically significant alterations with *P* value <0.05 using Mann-Whitney *U* test. Swept-source-OCTA metrics were acquired using Angio 6 × 6-mm acquisition protocol.

Six-Month Progression

Only 51 eyes completed the 2 examinations with an interval of 6 months. Twelve eyes (23.5%) were classified as DRSS level 43, 30 eyes (58.8%) classified as DRSS level 47, and 9 eyes (17.7%) as DRSS level 53.

Results showing the progression of retinal capillary hypoperfusion (ischemia) during the 6-month period follow-up using the SS-OCTA and the SD-OCTA are presented in [Table 2](#).

Swept-source-OCTA metrics showed statistically significant differences in the foveal avascular zone metrics (area:

Table 2. Six-month Progression in Eyes with Advanced Stages of NPDR

	SD-OCTA			SS-OCTA		
	Baseline	6 Mo	P Value	Baseline	6 Mo	P Value
	n = 51	n = 51	0 mo–6 mo	n = 51	n = 51	0 mo–6 mo
Ophthalmological examination 6 × 6-mm acquisition protocols, mean ± SD						
FAZ area (mm ²)	0.28 ± 0.11	0.27 ± 0.12	0.272	0.31 ± 0.17	0.46 ± 0.59	0.004*
FAZ length (mm)	2.21 ± 0.50	2.23±0.56	0.098	2.38 ± 0.82	3.13 ± 3.02	0.007*
FAZ circularity (a.u.)	0.70 ± 0.07	0.67±0.08	0.113	0.68 ± 0.11	0.61 ± 0.17	0.011*
Skeletonized vessel density – InR – SCP (mm ⁻¹)	16.48 ± 1.71	16.13 ± 1.57	0.068	18.10 ± 2.27	17.54 ± 1.76	0.001*
Skeletonized vessel density – InR – DCP (mm ⁻¹)	9.20 ± 3.04	8.25 ± 2.98	0.033*	10.79 ± 3.66	9.86 ± 3.40	0.084
Skeletonized vessel density – OutR – SCP (mm ⁻¹)	16.62 ± 1.34	16.09 ± 1.38	0.029*	18.30 ± 1.82	17.92 ± 1.54	0.003*
Skeletonized vessel density – OutR – DCP (mm ⁻¹)	10.58 ± 2.94	9.53 ± 3.01	0.022*	10.63 ± 3.57	9.57 ± 3.18	0.017*
Perfusion density – InR – SCP (a.u.)	0.40 ± 0.04	0.39 ± 0.04	0.063	0.39 ± 0.05	0.38 ± 0.04	0.001*
Perfusion density – InR – DCP (a.u.)	0.19 ± 0.07	0.17 ± 0.07	0.024*	0.22 ± 0.08	0.20 ± 0.07	0.074
Perfusion density – OutR – SCP (a.u.)	0.42 ± 0.03	0.40 ± 0.04	0.022*	0.41 ± 0.04	0.40 ± 0.03	0.011*
Perfusion density – OutR – DCP (a.u.)	0.22 ± 0.07	0.20 ± 0.07	0.022*	0.22 ± 0.07	0.19 ± 0.07	0.024*

a.u. = arbitrary units; DCP = deep capillary plexus; FAZ = foveal avascular zone; InR = inner ring; OutR = outer ring; SCP = superficial capillary plexus; SD = standard deviation; SD-OCTA = spectral-domain OCT angiography; SS-OCTA = swept-source OCT angiography.

*Values represent statistically significant alterations with *P* value <0.05 using Wilcoxon signed rank test.

P = 0.004, length: *P* = 0.007 and circularity: *P* = 0.011) and in both SVD and PD metrics for the inner ring (SCP, SVD: *P* = 0.001 and PD: *P* = 0.001) and outer ring areas (SCP, SVD: *P* = 0.003 and PD: *P* = 0.011; DCP, SVD: *P* = 0.017 and PD: *P* = 0.024). Spectral-domain OCTA also showed similar statistically significant differences but only in SVD and PD metrics for the inner and outer ring areas. It is noteworthy that the progression of capillary hypoperfusion during the 6-month period was identified by the SS-OCTA in eyes with DRSS levels 47 and 53 but not in DRSS level 43. These results are shown in Table 3 and Figure 1.

Discrimination between DRSS levels 43 from 47 was achieved when considering the MA formation rate in a 6-month interval (*P* = 0.047). In addition, differences between DRSS levels 47 and 53 for MA formation rate, MA disappearance rate, and MA turnover with 6-month interval were also identified but did not reach statistical significance. Six-month progression was also identified, in eyes with more severe stages of NPDR (DRSS levels 47 and 53), using a combination of capillary nonperfusion (SVD and PD) by performing SS-OCTA and MA counts using CFP images (Table 4).

No statistically significant differences were found in BCVA over the 6-month period of follow-up in the 3 DRSS levels included (baseline: 83.12 ± 5.29 letters vs. 6-month: 83.24 ± 5.29 letters, *P* = 0.262). Furthermore, no changes were also detected in structural metrics over the 6 months in central retinal thickness (baseline: 273.90 ± 25.68 μm vs. 6-month: 276.29 ± 30.60 μm, *P* = 0.326) and GCL + IPL thickness (baseline: 77.04 ± 11.15 μm vs. 6-month: 77.75 ± 10.59 μm, *P* = 0.702).

Finally, the number of IRMAs identified by SS-OCTA in the 6-month interval did not show significant differences.

Similar numbers were identified in the 6-month interval (baseline: 106 IRMA and 6-month: 98 IRMA).

Discussion

The results here reported show that OCTA can discriminate eyes with advanced stages of NPDR (DRSS levels 43, 47, and 53) and that, at this stage of the disease, it is possible to identify statistically significant differences within 6 months of retinal microvascular metrics while visual function remains stable. There is a progressive increase in capillary hypoperfusion (ischemia) identified using OCTA and in the most severe stage (DRSS level 53) there is a clear increase in the number of MAs identifiable by CFP. It is relevant that OCTA and fundus photography are both noninvasive imaging methods.

In previous studies, we have shown that in preclinical stage of retinopathy (eyes without visible lesions), the hypoperfusion stage is present in the central macula and predominantly in the SCP.³⁵ DR disease progression appears, therefore, to be characterized by an initial stage of increasing hypoperfusion involving initially the SCP with progressive involvement of the DCP and extending from the centre to the periphery (early stages of NPDR),^{11,36} followed by dominant hyperperfusion possibly because of the development of more dilated shunt vessels and finally IRMA which characterize DRSS levels 47 and 53 (advanced stages of NPDR).

Our results show that the capillary hypoperfusion in the DRSS levels 43 and 47 progresses by involving preferentially the DCP in the outer ring of the central retina until it appears to stabilize in the DRSS level 53. In contrast, the number of microaneurysms increases progressively through DRSS

Table 3. Six-month Progression by DR Severity Levels Using SS-OCTA

	DRSS Level 43			DRSS Level 47			DRSS Level 53		
	Baseline	6 Mo	P Value	Baseline	6 Mo	P Value	Baseline	6 Mo	P Value
	n = 12	n = 12	0 mo–6 mo	n = 30	n = 30	0 mo–6 mo	n = 9	n = 9	0 mo–6 mo
Ophthalmological examination SS-OCTA 6 × 6-mm acquisition protocol, mean ± SD									
FAZ area (mm ²)	0.36 ± 0.25	0.27 ± 0.09	0.204	0.31 ± 0.14	0.60 ± 0.74	<0.001*	0.25 ± 0.13	0.26 ± 0.16	0.359
FAZ length (mm)	2.63 ± 1.19	2.24 ± 0.44	0.339	2.36 ± 0.67	3.79 ± 3.80	<0.001*	2.09 ± 0.62	2.09 ± 0.76	0.652
FAZ circularity (a.u.)	0.65 ± 0.14	0.67 ± 0.09	0.622	0.69 ± 0.10	0.56 ± 0.19	<0.001*	0.68 ± 0.11	0.69 ± 0.08	0.652
Skeletonized vessel density – MAC – SCP (mm ⁻¹)	17.89 ± 2.46	18.31 ± 1.02	0.765	17.66 ± 1.67	17.09 ± 1.63	0.004*	19.30 ± 1.10	18.09 ± 1.38	0.039*
Skeletonized vessel density – MAC – DCP (mm ⁻¹)	10.41 ± 3.58	11.25 ± 1.60	0.898	9.65 ± 3.37	8.51 ± 3.36	0.056	12.79 ± 2.36	9.64 ± 2.79	0.039*
Skeletonized vessel density – InR – SCP (mm ⁻¹)	17.57 ± 3.33	18.43 ± 1.22	0.638	17.87 ± 1.85	16.94 ± 1.89	0.002*	19.61 ± 1.20	18.25 ± 1.19	0.023*
Skeletonized vessel density – InR – DCP (mm ⁻¹)	10.21 ± 4.11	11.57 ± 2.57	0.240	10.27 ± 3.67	9.13 ± 3.73	0.084	13.32 ± 1.68	9.87 ± 2.68	0.023*
Skeletonized vessel density – OutR – SCP (mm ⁻¹)	18.33 ± 2.21	18.59 ± 1.05	0.365	17.92 ± 1.69	17.50 ± 1.62	0.024*	19.52 ± 1.15	18.41 ± 1.54	0.039*
Skeletonized vessel density – OutR – DCP (mm ⁻¹)	10.85 ± 3.66	11.56 ± 1.43	0.831	9.80 ± 3.51	8.62 ± 3.43	0.067	13.08 ± 2.68	9.92 ± 2.98	0.055
Perfusion density – MAC – SCP (a.u.)	0.40 ± 0.06	0.41 ± 0.02	0.898	0.39 ± 0.04	0.38 ± 0.04	0.020*	0.43 ± 0.02	0.40 ± 0.03	0.016*
Perfusion density – MAC – DCP (a.u.)	0.21 ± 0.07	0.23 ± 0.03	0.765	0.20 ± 0.07	0.17 ± 0.07	0.067	0.26 ± 0.05	0.19 ± 0.06	0.055
Perfusion density – InR – SCP (a.u.)	0.38 ± 0.07	0.40 ± 0.03	0.413	0.39 ± 0.04	0.37 ± 0.04	0.002*	0.42 ± 0.02	0.39 ± 0.02	0.016*
Perfusion density – InR – DCP (a.u.)	0.20 ± 0.08	0.23 ± 0.05	0.278	0.21 ± 0.08	0.19 ± 0.08	0.067	0.27 ± 0.04	0.20 ± 0.05	0.016*
Perfusion density – OutR – SCP (a.u.)	0.41 ± 0.05	0.42 ± 0.02	0.638	0.40 ± 0.04	0.40 ± 0.04	0.123	0.44 ± 0.02	0.41 ± 0.03	0.016*
Perfusion density – OutR – DCP (a.u.)	0.22 ± 0.08	0.23 ± 0.03	1.000	0.20 ± 0.07	0.17 ± 0.07	0.063	0.27 ± 0.06	0.20 ± 0.06	0.055

a.u. = arbitrary units; DCP = deep capillary plexus; DRSS = Diabetic Retinopathy Severity Scale; FAZ = foveal avascular zone; InR = inner ring; MAC = macular area (20°); OutR = outer ring; SCP = superficial capillary plexus; SS-OCTA = swept-source OCT angiography.

*Values represent statistically significant alterations with *P* value <0.05 using Wilcoxon signed rank test.

Table 4. Combination of Microvascular Metrics Using SS-OCTA with MAT over a 6-month Period

Combining MAT with SS-OCTA metrics	DRSS Level 43		DRSS Level 47		DRSS Level 53		Pairwise Comparison			
	n = 12		n = 30		n = 9		DRSS Level 43 vs. DRSS Level 47		DRSS Level 47 vs. DRSS Level 53	
	β -value (CI)	P Value	β -value (CI)	P Value	β -value (CI)	P Value	Mean Change (CI)	P Value	Mean Change (CI)	P Value
SVD – SCP – inner ring + MAT	0.065 (–0.154 to 0.285)	0.559	0.040 (–0.012 to 0.092)	0.132	–0.021 (–0.037 to –0.006)	0.005*	–0.022 (–0.210 to 0.167)	0.822	–0.063 (–0.117 to –0.008)	0.024*
SVD – DCP – inner ring + MAT	0.074 (–0.241 to 0.388)	0.645	0.028 (–0.074 to 0.131)	0.591	–0.024 (–0.054 to 0.007)	0.131	–0.038 (–0.370 to 0.293)	0.822	–0.052 (–0.159 to 0.055)	0.340
SVD – SCP – outer ring + MAT	0.025 (–0.118 to 0.168)	0.735	0.019 (–0.028 to 0.065)	0.427	–0.026 (–0.041 to –0.011)	0.001*	–0.004 (–0.154 to 0.146)	0.960	–0.045 (–0.094 to 0.003)	0.068
SVD – DCP – outer ring + MAT	–0.059 (–0.272 to 0.155)	0.591	0.036 (–0.053 to 0.125)	0.422	–0.040 (–0.074 to –0.006)	0.022*	0.099 (–0.174 to 0.371)	0.478	–0.076 (–0.171 to 0.019)	0.115
PD – SCP – inner ring + MAT	0.002 (–0.003 to 0.006)	0.546	0.001 (0.000 to 0.002)	0.087	0.000 (–0.001 to 0.000)	0.034*	0.000 (–0.005 to 0.004)	0.847	–0.001 (–0.003 to 0.000)	0.024*
PD – DCP – inner ring + MAT	0.002 (–0.005 to 0.008)	0.646	0.001 (–0.001 to 0.003)	0.538	0.000 (–0.001 to 0.000)	0.168	–0.001 (–0.008 to 0.006)	0.847	–0.001 (–0.003 to 0.001)	0.322
PD – SCP – outer ring + MAT	0.001 (–0.003 to 0.004)	0.733	0.001 (0.000 to 0.002)	0.255	0.000 (–0.001 to 0.000)	0.017*	0.000 (–0.003 to 0.004)	0.945	–0.001 (–0.002 to 0.000)	0.066
PD – DCP – outer ring + MAT	–0.001 (–0.006 to 0.003)	0.586	0.001 (–0.001 to 0.003)	0.429	–0.001 (–0.001 to 0.000)	0.034*	0.002 (–0.004 to 0.008)	0.477	–0.002 (–0.003 to 0.000)	0.133

CI = confidence interval; DCP = deep capillary plexus; DRSS = Diabetic Retinopathy Severity Scale; MAT = microaneurysm turnover; PD = perfusion density; SCP = superficial capillary plexus; SS-OCTA = swept-source OCT angiography; SVD = skeletonized vessel density.

*Values represent statistically significant differences with P value <0.05 using linear mixed models to evaluate longitudinal changes (6-month) combining MAT with SS-OCTA metrics for each DRSS level and the post hoc analysis, where visit (0 month–6 month), DRSS levels (43, 47, and 53) and OCTA microvascular variables were used as fixed variables. SS-OCTA results were obtained from Angio 6 × 6-mm acquisition protocol.

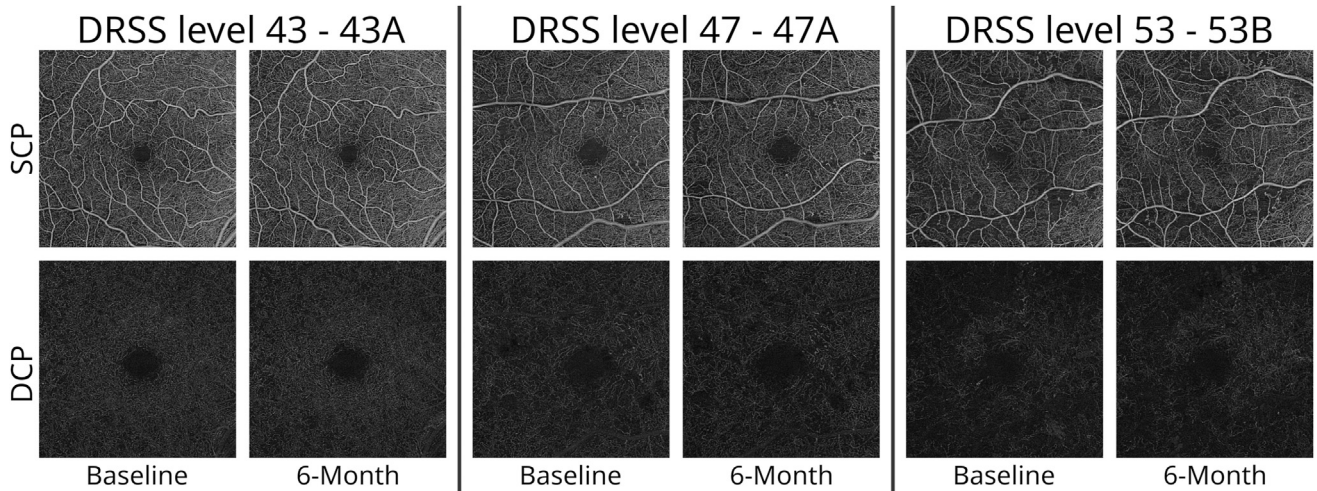


Figure 1. Superficial and deep capillary plexuses en face images acquired using swept-source OCT angiography PLEX Elite (6×6 -mm acquisition protocol) from patients with diabetic retinopathy severity levels 43, 47, and 53 in 6-month interval. DCP = deep capillary plexus; DRSS = Diabetic Retinopathy Severity Scale; SCP = superficial capillary plexus.

levels 43, 47, and 53 apparently in association with the presence of IRMA in DRSS levels 47 and 53. The observed pattern of disease progression from this study follows along the progression of DR suggested by Curtis et al.³⁷ A hypoperfusion stage followed by a hyperperfusion response.

Our baseline results show that when comparing different DRSS levels in this preproliferative stage of the disease, it is possible to discriminate them by using a combination of SS-OCTA metrics with MA counts. OCTA metrics identifying the progression in capillary closure (hypoperfusion – capillary occlusion) and the increase in MAs functioning as a surrogate for the development of dilated preferential shunts and IRMA (hyperperfusion – vasodilatation).^{18,38}

Our study also showed that the ischemic index obtained using UWF-FFA demonstrates the presence of capillary closure and hypoperfusion but is much less discriminative than the OCTA metrics obtained using the noninvasive SS-OCTA.³⁸ Furthermore, demarcating nonperfusion in FFA images is subjective, whereas OCTA metrics are automatically extracted.

In the proliferative stage of DR, it is crucial to be able to identify eyes at high risk of progression to vision loss. Curtis et al.³⁷ have proposed that in DR an initial phase of microvascular hypoperfusion (capillary occlusion) is followed by a shift to microvascular hyperperfusion (capillary occlusion). In this study, we were able to identify specific eyes/patients, where the predominant pathology is progressive ischemia and hypoperfusion,

followed by the presence of an abnormally increased flow response causing hyperperfusion identified by the presence of IRMA and increasing number of MAs.

In the current analysis, we found that progression of the preproliferative stage of DR can be detected based on retinal microvascular metrics obtained with OCTA, a noninvasive imaging procedure, in a 6-month interval. These results open the door for future interventional trials targeting retinal capillary closure and ischemia as well as addressing the subsequent hyperperfusion response.

One of the major limitations of RICHARD study is the small number of eyes with unbalanced DR groups ($N = 60$ eyes). Moreover, these patients have relatively well controlled type 2 diabetes. However, this last limitation, can be seen as an advantage as it minimizes the influence of systemic variables. Other relevant limitation is the reproducibility and repeatability of microvascular metrics using different OCTA devices and different protocols in same OCTA device.

The ability to monitor the balance between the initial hypoperfusion stage and the hyperperfusion response using metrics of capillary perfusion obtained with noninvasive OCTA imaging and MA counting open ways to predict risk of progression to PDR in a given eye, with moderate-severe nonproliferative retinopathy and offers data on which viable clinical trials can be designed to test new therapeutic agents to prevent nonproliferative stages of DR to progress to vision-threatening complications.

Footnotes and Disclosures

Originally received: June 25, 2024.

Final revision: August 2, 2024.

Accepted: October 7, 2024.

Available online: October 16, 2024. Manuscript no. XOPS-D-24-00204R1.

¹ AIBILI - Association for Innovation and Biomedical Research on Light and Image, Coimbra, Portugal.

² Coimbra Ophthalmology Reading Centre (CORC), Coimbra, Portugal.

³ Coimbra Institute for Clinical and Biomedical Research (iCBR), Faculty of Medicine, University of Coimbra, Portugal.

⁴ Eye Clinic, University Hospital Basel, Basel, Switzerland.

⁵ Boehringer Ingelheim, GmbH, Ingelheim am Rhein, Germany.

⁶ Center for Translational Health and Medical Biotechnology Research (TBIO)/Health Research Network (RISE-Health), ESS, Polytechnic of Porto, Porto, Portugal.

⁷ Institute of Ophthalmology, University College London, London, United Kingdom.

⁸ Faculty of Medicine, University of Coimbra, Coimbra, Portugal.

Disclosures:

All authors have completed and submitted the ICMJE disclosures form.

The author(s) have made the following disclosure(s):

I.P.M.: Support – Boehringer Ingelheim.

D.R.-F.: Support – Boehringer Ingelheim.

T.S.: Support – Boehringer Ingelheim.

L.M.: Support – Boehringer Ingelheim.

A.C.V.-M.: Support – Boehringer Ingelheim.

T.C.N.Y.: Support – Boehringer Ingelheim; Travel support – Boehringer Ingelheim; Employee – Boehringer Ingelheim.

A.R.S.: Support – Boehringer Ingelheim.

E.P.: Previous employee – Boehringer Ingelheim.

J.C.-V.: Support – Boehringer Ingelheim; Grants – Bayer, Boehringer Ingelheim, Carl Zeiss Meditec; Consultant – Alimera Sciences, Bayer, Boehringer Ingelheim, Carl Zeiss Meditec, Roche.

The other authors have no proprietary or commercial interest in any materials discussed in this article.

Supported by an IIR Grant from Boehringer Ingelheim International GmbH. Boehringer Ingelheim reviewed and approved this manuscript and decision to submit the manuscript for publication.

HUMAN SUBJECTS: Human subjects were included in this study. The RICHARD study (NCT05112445, clinicaltrials.gov identifier) is a non-interventional prospective cohort study with 2 years of follow-up period and adheres to the tenets of the Declaration of Helsinki. This study was reviewed and approved by the Association for Innovation and Biomedical Research on Light and Image Ethics Committee and was conducted in

accordance with the legislation and institutional requirements. The participants provided their written informed consent to participate in this study.

No animal subjects were used in this study.

Author Contributions:

Conception and design: Marques, A.R. Santos, Pearce, Cunha-Vaz

Data collection: Marques, Reste-Ferreira, T. Santos, Mendes, Martinho, A.R. Santos

Analysis and interpretation: Marques, Reste-Ferreira, T. Santos, Mendes, Martinho, Yamaguchi, A.R. Santos, Pearce, Cunha-Vaz

Obtained funding: Cunha-Vaz

Overall responsibility: Marques, Reste-Ferreira, T. Santos, Mendes, Martinho, Yamaguchi, A.R. Santos, Pearce, Cunha-Vaz

Abbreviations and Acronyms:

BCVA = best-corrected visual acuity; **CFP** = color fundus photography; **CSME** = clinically significant macular edema; **DCP** = deep capillary plexus; **DR** = diabetic retinopathy; **DRSS** = Diabetic Retinopathy Severity Scale; **GCL** = ganglion cell layer; **IPL** = inner plexiform layer; **IRMA** = intraretinal microvascular abnormality; **MA** = microaneurysm; **NPDR** = nonproliferative diabetic retinopathy; **OCTA** = OCT angiography; **PD** = perfusion density; **PDR** = proliferative diabetic retinopathy; **SCP** = superficial capillary plexus; **SD-OCTA** = spectral-domain OCT angiography; **SS-OCTA** = swept-source OCT angiography; **SVD** = skeletonized vessel density; **UWF** = ultrawidefield; **UWF-FP** = ultrawidefield fundus photography; **UWF-FFA** = ultrawidefield fundus fluorescein angiography.

Keywords:

Diabetic retinopathy, Hypoperfusion, Hyperperfusion, Progression, Microaneurysm.

Correspondence:

José Cunha-Vaz, MD, PhD, AIBILI, Edifício Prof. Doutor José Cunha-Vaz, Azinhaga Sta. Comba, Celas, 3000-548 Coimbra, Portugal. E-mail: cunhavaz@aibili.pt.

References

- Aiello LM. Perspectives on diabetic retinopathy. *Am J Ophthalmol*. 2003;136:122–135.
- Narayan KMV, Boyle JP, Geiss LS, et al. Impact of recent increase in incidence on future diabetes burden: U.S., 2005–2050. *Diabetes Care*. 2006;29:2114–2116.
- Diabetes Federation International. *IDF Diabetes Atlas*. 10th ed. Brussels, Belgium: International Diabetes Federation; 2021.
- Cheung N, Mitchell P, Wong TY. Diabetic retinopathy. *Lancet*. 2010;376:124–136.
- Yau JWY, Rogers SL, Kawasaki R, et al. Global prevalence and major risk factors of diabetic retinopathy. *Diabetes Care*. 2012;35:556–564.
- Marques IP, Kubach S, Santos T, et al. Optical coherence tomography angiography metrics monitor severity progression of diabetic retinopathy—3-year longitudinal study. *J Clin Med*. 2021;10:2296. <https://doi.org/10.3390/jcm10112296>.
- Marques IP, Ribeiro ML, Santos TP, et al. Different risk profiles for progression of nonproliferative diabetic retinopathy: a 2-year study. *Ophthalmol Ther*. 2023;12:485–500.
- Cunha-Vaz J. A central role for ischemia and OCTA metrics to follow DR progression. *J Clin Med*. 2021;10:1821. <https://doi.org/10.3390/jcm10091821>.
- Reste-Ferreira D, Santos T, Marques IP, et al. Characterization of central-involved diabetic macular edema using OCT and OCTA. *Eur J Ophthalmol*. 2024;11206721241248478. <https://doi.org/10.1177/11206721241248478>.
- Silva PS, Cavallerano JD, Sun JK, et al. Peripheral lesions identified by mydriatic ultrawide field imaging: distribution and potential impact on diabetic retinopathy severity. *Ophthalmology*. 2013;120:2587–2595.
- Santos AR, Almeida AC, Rocha AC, et al. Central and peripheral involvement of the retina in the initial stages of diabetic retinopathy. *Retina*. 2024;44:700–706.
- Marques IP, Alves D, Santos T, et al. Multimodal imaging of the initial stages of diabetic retinopathy: different disease pathways in different patients. *Diabetes*. 2019;68:648–653.
- Marques IP, Madeira MH, Messias AL, et al. Different retinopathy phenotypes in type 2 diabetes predict retinopathy progression. *Acta Diabetol*. 2021;58:197–205.
- Flaxel CJ, Adelman RA, Bailey ST, et al. Diabetic retinopathy preferred practice pattern. *Ophthalmology*. 2020;127:P66–P145.
- Spaide RF, Klancnik JM, Cooney MJ. Retinal vascular layers imaged by fluorescein angiography and optical coherence tomography angiography. *JAMA Ophthalmol*. 2015;133:45–50.
- Schaal KB, Munk MR, Wyssmueller I, et al. Vascular abnormalities in diabetic retinopathy assessed with swept-source optical coherence tomography angiography widefield imaging. *Retina*. 2019;39:79–87.

17. Santos T, Warren LH, Santos AR, et al. Swept-source OCTA quantification of capillary closure predicts ETDRS severity staging of NPDR. *Br J Ophthalmol*. 2022;106:712–718.
18. Santos AR, Mendes L, Madeira MH, et al. Microaneurysm turnover in mild non-proliferative diabetic retinopathy is associated with progression and development of vision-threatening complications: A 5-year longitudinal study. *J Clin Med*. 2021;10:2142. <https://doi.org/10.3390/jcm10102142>.
19. Sjølie AK, Klein R, Porta M, et al. Retinal microaneurysm count predicts progression and regression of diabetic retinopathy. Post-hoc results from the DIRECT Programme. *Diabet Med*. 2011;28:345–351.
20. Ferris FL, Bailey I. Standardizing the measurement of visual acuity for clinical research studies: guidelines from the Eye Care Technology Forum. *Ophthalmology*. 1996;103:181–182.
21. Treatment E, Retinopathy D. Grading diabetic retinopathy from stereoscopic color fundus photographs—an extension of the modified Airlie House classification. ETDRS Report Number. 10. Early Treatment Diabetic Retinopathy Study Research Group. *Ophthalmology*. 1991;98:786–806.
22. Domalpally A, Barrett N, Reimers J, Blodi B. Comparison of ultra-widefield imaging and standard imaging in assessment of early treatment diabetic retinopathy severity scale. *Ophthalmol Sci*. 2021;1:100029. <https://doi.org/10.1016/j.xops.2021.100029>.
23. Duncan N, Barrett N, Schildroth K, et al. Comparison of standard 7-field, Clarus, and Optos ultrawidefield imaging systems for diabetic retinopathy (COCO Study). *Ophthalmol Sci*. 2024;4:100427. <https://doi.org/10.1016/j.xops.2023.100427>.
24. Lee J, Sagong M. Ultra-widefield retina imaging: principles of technology and clinical applications. *J Retin*. 2016;1:1–10.
25. Manivannan A, Plskova J, Farrow A, et al. Ultra-wide-field fluorescein angiography of the ocular fundus. *Am J Ophthalmol*. 2005;140:525–527.
26. Jiang AC, Srivastava SK, Hu M, et al. Quantitative ultra-widefield angiographic features and associations with diabetic macular edema. *Ophthalmol Retin*. 2020;4:49–56.
27. Lei J, Durbin MK, Shi Y, et al. Repeatability and reproducibility of superficial macular retinal vessel density measurements using optical coherence tomography angiography en face images. *JAMA Ophthalmol*. 2017;135:1092–1098.
28. Durbin MK, An L, Shemonski ND, et al. Quantification of retinal microvascular density in optical coherence tomographic angiography images in diabetic retinopathy. *JAMA Ophthalmol*. 2017;135:370–376.
29. Foote KG, Roorda A, Duncan JL. Multimodal imaging in choroïderemia. *Adv Exp Med Biol*. 2019;1185:139–143.
30. Akman A, Meditec CZ. Optical coherence tomography in glaucoma. *Opt Coherence Tomogr Glaucoma*. 2018:27–37.
31. Li Y, El Habib Daho M, Conze PH, et al. Hybrid fusion of high-resolution and ultra-widefield OCTA acquisitions for the automatic diagnosis of diabetic retinopathy. *Diagnostics*. 2023;13:2770. <https://doi.org/10.3390/diagnostics13172770>.
32. Kakihara S, Hirano T, Kitahara J, et al. Application of optical coherence tomography angiography to assess systemic severity in patients with hereditary transthyretin amyloidosis. *PLOS ONE*. 2022;17:1–12.
33. Nunes S, Pires I, Rosa A, et al. Microaneurysm turnover is a biomarker for diabetic retinopathy progression to clinically significant macular edema: findings for type 2 diabetics with nonproliferative retinopathy. *Ophthalmologica*. 2009;223:292–297.
34. Bernardes R, Nunes S, Pereira I, et al. Computer-assisted microaneurysm turnover in the early stages of diabetic retinopathy. *Ophthalmologica*. 2009;223:284–291.
35. Santos T, Santos AR, Almeida AC, et al. Retinal capillary nonperfusion in preclinical diabetic retinopathy. *Ophthalmic Res*. 2023;66:1327–1334.
36. Marques IP, Ribeiro ML, Santos T, et al. Patterns of progression of nonproliferative diabetic retinopathy using non-invasive imaging. *Transl Vis Sci Technol*. 2024;13:22. <https://doi.org/10.1167/tvst.13.5.22>.
37. Curtis TM, Gardiner TA, Stitt AW. Microvascular lesions of diabetic retinopathy: clues towards understanding pathogenesis? *Eye*. 2009;23:1496–1508.
38. Vujosevic S, Fantaguzzi F, Silva PS, et al. Macula vs periphery in diabetic retinopathy: OCT-angiography and ultra-wide field fluorescein angiography imaging of retinal non perfusion. *Eye*. 2024;38:1668–1673.